Ferromagnetism and the metal-insulator transition in the thiospinel Cu(Ir1-xCrx)2S4

Ferromagnetism and the metal-insulator transition in the thiospinel $Cu(Ir_{1-x}Cr_x)_2S_4$

Ryo Endoh, Junji Awaka, and Shoichi Nagata*
Department of Materials Science and Engineering, Muroran Institute of Technology, 27-1 Mizumoto-cho, Muroran, Hokkaido, 050-8585 Japan

(Received 7 January 2003; revised manuscript received 30 April 2003; published 16 September 2003)

A thiospinel $CuIr_2S_4$ exhibits a temperature-induced metal-insulator (M-I) transition at 230 K with a simultaneous spin-dimerization and charge-ordering transition although a three-dimensional system. On the other hand, $CuCr_2S_4$ has the same spinel structure without any structural transformations. $CuCr_2S_4$ remains metallic and is ferromagnetic with the Curie temperature $T_C \simeq 377$ K. In order to see the effect of substituting Cr for Ir on the M-I transition, we have carried out a systematic experimental study of electrical and magnetic properties of $Cu(Ir_{1-x}Cr_x)_2S_4$ system. The M-I transition temperature decreases steeply with increasing Cr-composition x and this transition is not detected above $x \simeq 0.05$. The value of T_C decreases with decreasing x from 1.0, then T_C disappears below $x \simeq 0.20$. The ferromagnetic state suggests the non-collinear spin alignment. In the intermediate composition range over $x = 0.08$ to 0.20, the B-site undergoes a local crystal distortion around 180 K, where the energy level t_{2g} splits into lower symmetry. Then the low-spin state within the t_{2g} subspace is realized for Cr^{3+} ion with $s = 1/2$. The magnetic state of Cr^{3+} ion indicates a crossover from high temperature $s = 3/2$ to low temperature $s = 1/2$ state around 180 K.

DOI: 10.1103/PhysRevB.68.115106 PACS number(s): 71.30.+h, 75.50.−y, 75.30.Cr, 72.80.Ga

I. INTRODUCTION

Investigations of the metal-insulator (M-I) transition in $CuIr_2S_4$ and related investigations have been extensively made in the last decade.[1–54] This compound $CuIr_2S_4$ has a spinel structure where Cu ions occupy the A (tetrahedral) sites and Ir ions occupy the B (octahedral) sites. $CuIr_2S_4$ exhibits a temperature-induced M-I transition around $T_{M\text{-}I} = 230$ K with structural transformation, showing hysteresis on heating and cooling. The resistivity of $CuIr_2S_4$ varies abruptly by nearly three orders of magnitude at $T_{M\text{-}I}$. The behavior changes from metallic above $T_{M\text{-}I}$ to semiconductive below $T_{M\text{-}I}$. The temperature dependence of magnetic susceptibility exhibits a steplike anomaly corresponding to the M-I transition. In the insulating phase, monovalent Cu^+ ion has been verified by Cu nuclear magnetic resonance and photoemission measurements.[7,11] A significant characteristic feature is the absence of localized magnetic moment below $T_{M\text{-}I}$. Detailed crystallographic structural analysis of the low temperature phase has been made.[27,40,42,43,48] Their results indicate that $CuIr_2S_4$ is a rare and possibly unique example of a three-dimensional compound displaying a spin-dimerization transition, which occurs simultaneously with charge ordering.[48] The majority of electrical carriers in the semiconductive (insulating) phase is holes, which is confirmed by Hall effect measurements. Carrier concentrations of 10^{20} cm^{-3} in the insulating phase and of 10^{22} cm^{-3} in the metallic phase are observed.[21]

$CuCr_2S_4$ also has spinel structure and shows a metallic conductivity. $CuCr_2S_4$ is ferromagnetic with a Curie temperature $T_C \simeq 377$ K.[55–76] The formula unit has a net magnetic moment close to $5\mu_B$. Lotgering and co-workers[56,57,64,72] proposed that the mixed valence model of Cr ion has been shown as $Cu^+Cr^{3+}Cr^{4+}S_4^{2-}$; here the Cr^{3+} ion has $3\mu_B$ and the Cr^{4+} ion has $2\mu_B$, and a Cu^+ ion has the closed shell, where all the Cr ions align parallel each other; as a result the formula unit of $CuCr_2S_4$ has a net magnetic moment of $5\mu_B$. The metallic conduction and the ferromagnetism have been attributed to double exchange between Cr^{3+} and Cr^{4+} ions.[56,57,64,72,76] This interpretation has been verified experimentally by recent precise magnetic circular dichroism in the soft x-ray absorption spectra.[74] Kimura *et al.*[74] pointed out that the spin magnetic moment of Cu site in $CuCr_2S_4$ is as large as $0.078\mu_B$ per Cu atom.

On the other hand, Goodenough[61,63] has explained that the ionic configuration of $CuCr_2S_4$ can be described schematically $Cu^{2+}Cr_2^{3+}S_4^{2-}$, as two Cr^{3+} ions where three electrons in the $3d$ shell with spin up, and a Cu^{2+} ion which is aligned antiparallel to that of Cr^{3+}. Each Cr^{3+} ion has a moment of $3\mu_B$ and each Cu^{2+} ion has a moment of $1\mu_B$ in the opposite direction. Consequently the formula unit of $CuCr_2S_4$ has a net magnetic moment of $5\mu_B$.

We have successfully synthesized the single phase $Cu(Ir_{1-x}Cr_x)_2S_4$ specimens and carried out a systematic experimental study of structural, electrical, and magnetic properties of $Cu(Ir_{1-x}Cr_x)_2S_4$. The increase of Cr composition x leads to a remarkable change in the magnetic and electrical features. A phase diagram between temperature T versus Cr composition x has been obtained experimentally for this system in the present study.

II. EXPERIMENTAL METHODS

The polycrystalline specimens were prepared by a solid-state reaction. Mixtures of high-purity fine powders of Cu (purity 99.99%), Ir (99.99%), Cr (99.99%), and S (99.999%) with nominal stoichiometry were heated in sealed quartz tubes to 1123 K and kept at this temperature for ten days. The resultant powder specimens were reground and pressed to rectangular bars at a pressure of 0.2 GPa and then were heated to 1123 K for two days. For a higher Cr composition $0.50 \leqslant x \leqslant 1.00$, the high-purity specimens were obtained by regrinding and repeating the process of the heat treatment.

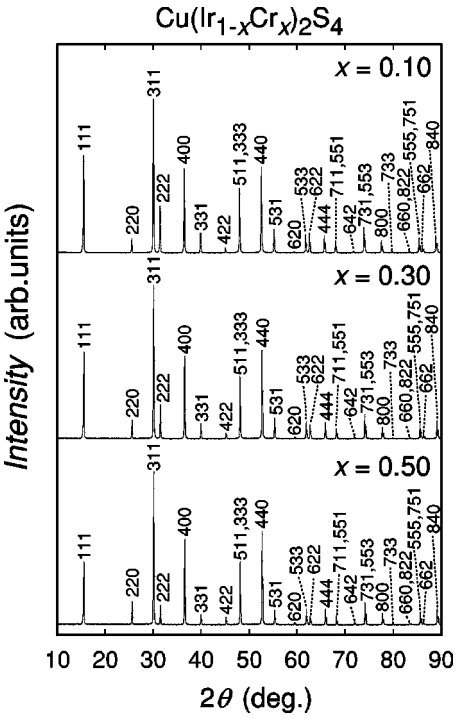

FIG. 1. Powder x-ray diffraction patterns for $x=0.10$, 0.30, and 0.50 at room temperature.

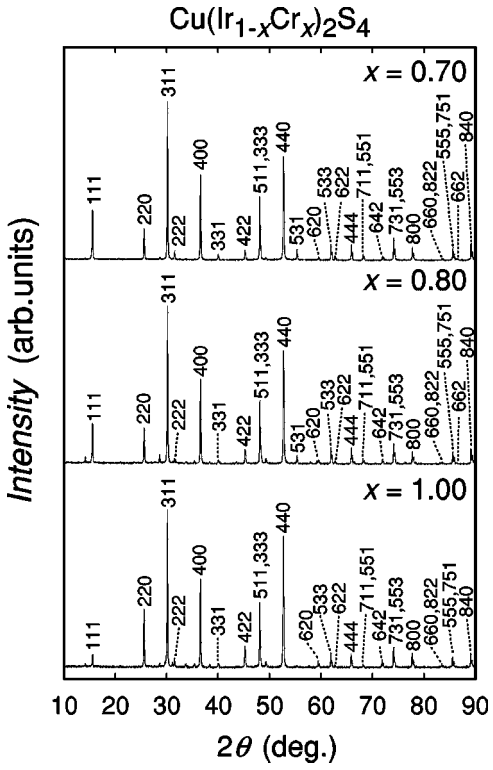

FIG. 2. Powder x ray diffraction patterns for $x=0.70$, 0.80, and 1.00 at room temperature.

The study of a higher value of the Cr composition x than 0.70 has the disadvantage that the preparation of single phase samples is more difficult. The identification of the crystal structure and the determination of lattice constants were carried out by the powder x-ray diffraction method using Cu Kα radiation from room temperature to $\simeq$80 K. A single crystal of $CuCr_2S_4$ ($x=1.00$) has been successfully grown by a chemical vapor transport method, and the magnetic properties have been measured using these single crystals. The resistivity ρ of sintered specimens with dimensions of about $2\times2\times10$ mm^3 was measured over a temperature range between 4.2 K and room temperature. The dc magnetic susceptibility and the magnetization curve were measured with a Quantum Design superconducting quantum interference device (rf-SQUID) magnetometer.

III. RESULTS AND DISCUSSION

A. Structural transformation

A spinel-type structure was confirmed for all the samples of $Cu(Ir_{1-x}Cr_x)_2S_4$, as can be seen in Figs. 1 and 2. The value of unit cell parameter a, obtained by the least square method, varies as shown in Fig. 3 at room temperature, where a does not obey Vegard's law. The unit cell size a decreases with Cr substitution to a broad minimum around $x=0.50$; then this value a increases from $x=0.50$ to 1.00. The ionic radius of Cr is smaller than that of Ir for the same valence. A similar behavior, for the variation of the lattice constant, has been observed in $Cu(Ir_{1-x}Ti_x)_2S_4$,[51] $Cu(Ir_{1-x}V_x)_2S_4$,[77] and $Cu(Rh_{1-x}Cr_x)_2S_4$ (Ref. 70) systems. The two effects might be superimposed, that is, the average ionic radius may decrease with x obeying Vegard's law, and the difference in the cohesive energy in the d band. The latter is related to the delocalized nature of d electrons in $Cu(Ir_{1-x}Cr_x)_2S_4$ which could result in the strong cohesive energy difference due to the different occupation numbers of d electrons for Cr and Ir in the d band. Here let us consider the simplified energy band model of simple metallic elements instead of a complicated compound. This simple model predicts that the half-filled state gives the highest cohesive energy in the d band. Therefore, the atomic radius in the metallic bond has a tendency toward the minimum for a half-filled d band. The magnitude of the shrinkage for the unit cell size, then, grows at the half-filled occupation num-

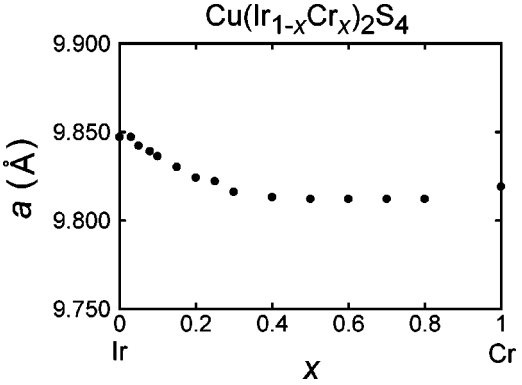

FIG. 3. The lattice constant a as a function of Cr composition x at room temperature.

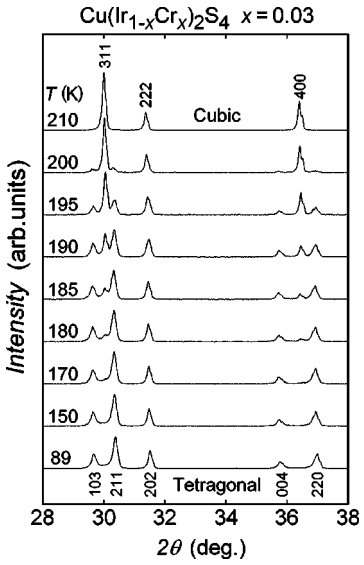

FIG. 4. Temperature dependence of the powder x-ray diffraction pattern for $x=0.03$ upon heating.

ber in the *d* band in order to gain a cohesive energy with spreading *d*-band-width. It is noted that the basic characteristics could originate from the difference in cohesive energy due to the diferent occupation numbers of the *d* electrons for Cr and Ir ions. Presumably, the marked anomalous behavior of *a* versus *x* can be observed manifestly only for the restricted situation where the number of *d* electron is extremely different such as $Cu(Ir_{1-x}M_x)_2S_4$; $M=$Ti, V, and Cr.

Figure 4 shows the powder x-ray diffraction patterns of the sample with $x=0.03$ at various temperatures near $T_{M\text{-}I}$. The structural transformation is observed from cubic to tetragonal symmetry with decreasing temperature. At 210 K, the diffraction peaks can be indexed with cubic symmetry with the space group $Fd\bar{3}m$. Between 180 and 200 K, the coexistence of cubic and tetragonal symmetries can be seen,

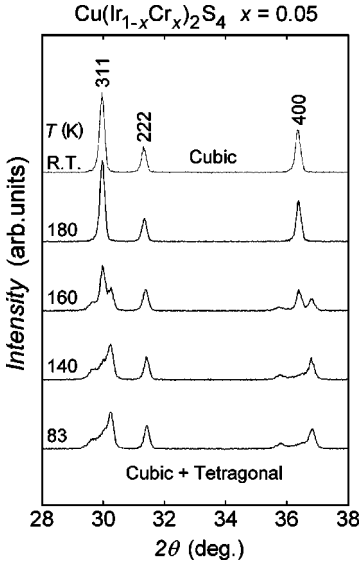

FIG. 5. Temperature dependence of the powder x-ray diffraction pattern for $x=0.05$ upon heating.

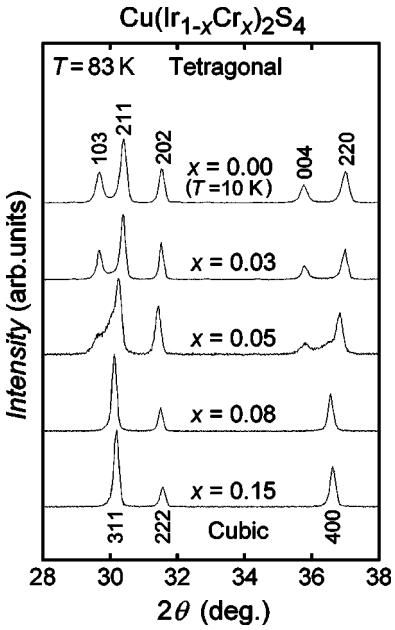

FIG. 6. X-ray diffraction pattern for $0.00\leqslant x\leqslant 0.15$ at 83 K over the angle range $28\leqslant 2\theta\leqslant 38°$.

where two peaks from cubic symmetry and three from tetragonal symmetry overlap in the diffraction angle region $29\leqslant 2\theta\leqslant 32°$. One peak arises from the cubic and two from the tetragonal overlap in the region $35\leqslant 2\theta\leqslant 37°$. The diffraction peaks at 150 K are indexed with the tetragonal symmetry with the space group $I4_1/amd$. The temperature of the structural transformation corresponds fairly well to the midpoint of the abrupt increase in the resistivity, which also coincides with that of the susceptibility. Figure 5 shows the powder x-ray diffraction patterns of the sample $x=0.05$ at various temperature.

Figure 6 presents the composition dependence of diffraction patterns over the range $0.00\leqslant x\leqslant 0.15$ at a constant temperature of 83 K. Specimens with $x=0.00$ and 0.03 have a tetragonal structure at 83 K. For the specimen with $x=0.05$, there exist both tetragonal and cubic phases. The

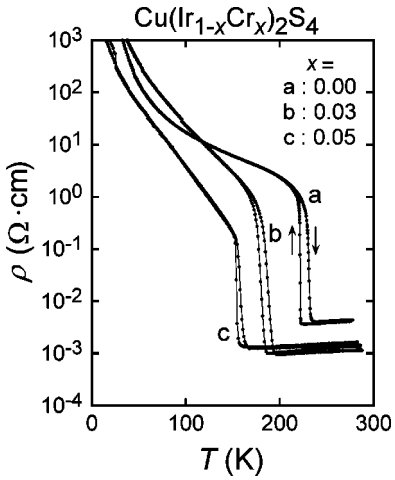

FIG. 7. Temperature dependence of the electrical resistivity ρ for sintered $Cu(Ir_{1-x}Cr_x)_2S_4$ specimens for $0.00\leqslant x\leqslant 0.05$.

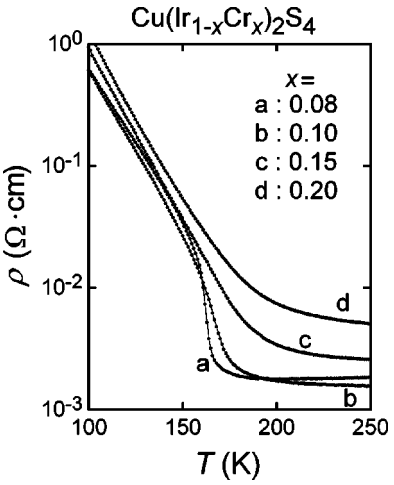

FIG. 8. Temperature dependence of the electrical resistivity ρ for sintered $Cu(Ir_{1-x}Cr_x)_2S_4$ specimens for $0.08 \leqslant x \leqslant 0.20$.

specimens with $x=0.08$ and 0.15 have only cubic phases. We presume that this coexistence of cubic and tetragonal symmetries exists on a rather microscopic scale and that these two phases mix homogeneously, each providing a percolation system. The dissociation between two phases may not be developed in the macroscopic region. This conjecture is indirectly supported by the macroscopic results that the temperature dependence of the resistivity and magnetic susceptibility vary not irregularly but fairly smoothly over a wide composition region.

B. Variation of metal-insulator transition in $Cu(Ir_{1-x}Cr_x)_2S_4$

The temperature dependences of electrical resistivity ρ are shown in Figs. 7 and 8. The sample of $x=0.10$ does not show a sharp jump in the resistivity, as indicated in Fig. 8. For $x=0.15$, the temperature dependence of the resistivity is semiconductive in all measured temperature ranges. Since the resistive jump becomes ill defined, the precise value of $T_{M\text{-}I}$ is not clear. Figure 9 presents the data for $0.30 \leqslant x \leqslant 0.80$. The resistivity ρ with $x \geqslant 0.60$ indicates rather less temperature dependence, and ρ with $x=0.80$ is flattened out between 4.2 K and room temperature; then the metallic state is recovered for $x \geqslant 0.80$. The metallic state of the pure $CuCr_2S_4$ compound[70,75] is consistent with the result of our present study.

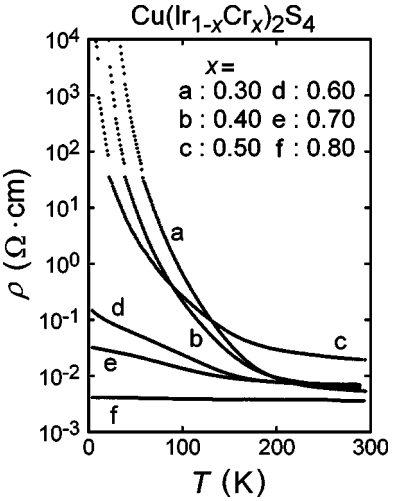

FIG. 9. Temperature dependence of the electrical resistivity ρ for sintered $Cu(Ir_{1-x}Cr_x)_2S_4$ specimens for $0.30 \leqslant x \leqslant 0.80$.

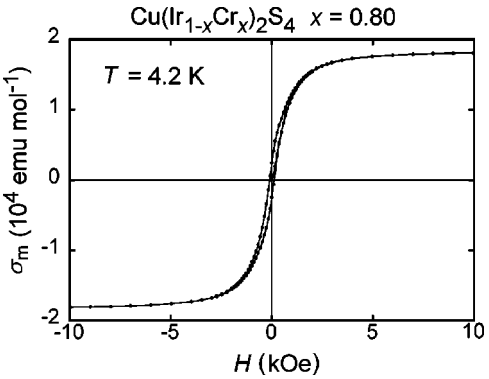

FIG. 10. Magnetization curve up to 10.000 kOe for $x=0.80$ at 4.2 K.

C. Variation of the ferromagnetism

As a representative result, the magnetization curve for $x=0.80$ at 4.2 K is shown in Fig. 10. The demagnetizing field corrections for this M-H curve have not been made. This sample shows a narrow hysteresis loop and an almost saturated behavior at a higher magnetic field. Figure 11 shows the magnetization curves at 4.2 K for specimens with various compositions x. The temperature dependences of the magnetization M at a constant magnetic field of $H=10.000$ kOe are indicated in Fig. 12. The magnitude of the magnetization at 4.2 K increases with increasing Cr composition x. Figure 13 shows the inverse susceptibility χ^{-1} versus T for $x=0.50$ in the paramagnetic temperature region $T \geqslant 150$ K. Here, the susceptibility is defined as $\chi=M/H$. The inverse susceptibility versus T curve is shifted upward from the line predicted by the Curie-Weiss law, which should reflect a tendency toward short range order. The solid line obeys the Curie-Weiss law well. The values of an asymptotic Curie temperature θ_p for the ferromagnet is 138 K. The inset in Fig. 13 shows a temperature derivative dM/dT curve at H

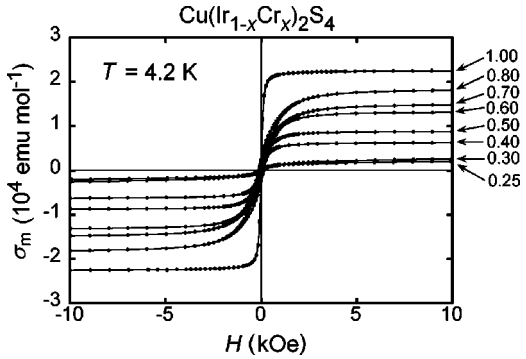

FIG. 11. Magnetization curve up to 10.000 kOe for $0.25 \leqslant x \leqslant 1.00$ at 4.2 K.

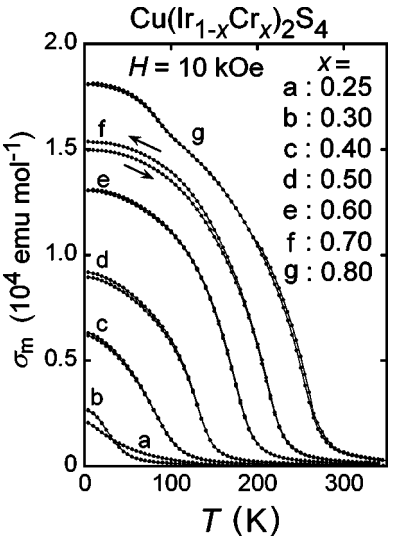

FIG. 12. Temperature dependences of magnetization for $Cu(Ir_{1-x}Cr_x)_2S_4$ at a constant field of 10.000 kOe for $0.25 \leqslant x \leqslant 0.80$.

$=10.000$ kOe as a function of temperature for $x=0.50$. The temperature at the negative peak of the dM/dT curve is approximately 130 K. This inflection points correspond essentially to the Curie point of the ferromagnetic state, which indicates the disappearance of the spontaneous magnetization. The value of θ_p in Fig. 13 is somewhat larger than that of the negative peak of dM/dT.

D. Magnetic susceptibility

The susceptibility shows a steplike anomaly at $T_{M\text{-}I}$ for $CuIr_2S_4$. For lower composition specimens with $x \leqslant 0.15$, a steplike anomaly is found in both ρ and χ. For $x=0.15$, the temperature hysteresis is not observed in ρ and χ. The Curie-Weiss behavior of the magnetic susceptibility below and above $T_{M\text{-}I}$ arises from the substitution of Cr for Ir. The gradual variation of the susceptibility with x implies that the Cr ion introduces the localized magnetic moments. Figure 14 displays the magnetic susceptibility, emphasizing the high temperature data for an intermediate composition region.

Figure 15 presents the inverse magnetic susceptibility for

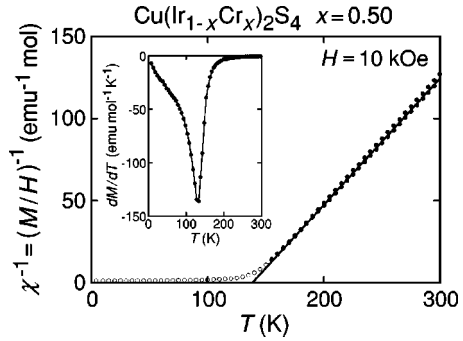

FIG. 13. Temperature dependence of the inverse susceptibility $\chi^{-1}=(M/H)^{-1}$ for $x=0.50$. Temperature derivative dM/dT as a function of temperature for $x=0.50$ is indicated in the inset.

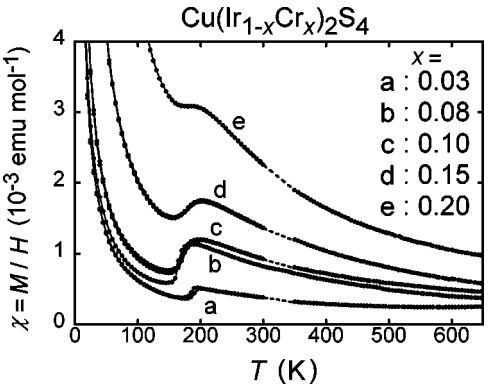

FIG. 14. High temperature magnetic susceptibility vs temperature of $Cu(Ir_{1-x}Cr_x)_2S_4$ for $0.03 \leqslant x \leqslant 0.20$. The applied magnetic field is 10.000 kOe.

the specimen with $x=0.08$. The susceptibility can be fitted to a modified Curie-Weiss law, $\chi=C/(T-\theta)+\chi_0$, where χ_0 is the temperature independent term, C the Curie constant, and θ the Weiss temperature. Table I shows the summary of the magnetic data. The value of effective magnetic moment μ_{eff}/Cr-ion indicates that only Cr ions possess a localized magnetic moment, while Cu, Ir, and S ions have no magnetic moments.

The broad humps are found around $T^{\star} \cong 180$ K in Fig. 14. These humps are basically the traces of the M-I transition observed in the lower composition x. The intermediate com-

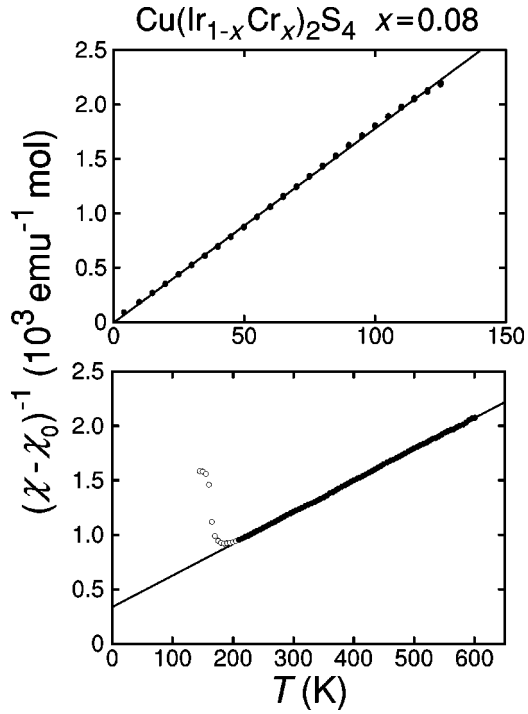

FIG. 15. Temperature dependence of the inverse susceptibility $(\chi-\chi_0)^{-1}=(M/H)^{-1}$ for $x=0.08$ between 4.2 and 130 K (above), and also between 200 and 600 K (below). Here, the value of χ_0 is different between two graphs.

TABLE I. Summary of the magnetic properties of $Cu(Ir_{1-x}Cr_x)_2S_4$ for $0.00 \leqslant x \leqslant 0.20$. These numerical values are extracted from the magnetic susceptibility based on the modified Curie-Weiss law. The effective magnetic moment $\mu_{\rm eff}$/Cr-ion indicates that only Cr ions possess a localized magnetic moment, while Cu, Ir and S ions have no magnetic moment. The value of T^* is approximately 180 K; see the text. The value of χ_0 includes appreciable experimental errors.

Curie - Weiss law ($T<T^*$)						
x	χ_0 (emu mol^{-1})	C (emu K/mol-f.u.)	θ (K)	$\mu_{\rm eff}=g\sqrt{J(J+1)}\cong 2\sqrt{S(S+1)}$		Temperature
				(μ_B / mol-f.u.)	(μ_B / Cr-ion)	
0.00						
0.03	-0.823×10^{-5}	0.05465	0.004	0.661	2.70	$4.2 \leqslant T \leqslant 165$ K
0.05	0.543×10^{-4}	0.05337	0.653	0.653	2.07	$4.2 \leqslant T \leqslant 140$ K
0.08	0.772×10^{-4}	0.05606	0.430	0.670	1.67	$4.2 \leqslant T \leqslant 130$ K
0.10	0.878×10^{-4}	0.08560	-0.204	0.832	1.86	$4.2 \leqslant T \leqslant 120$ K
0.15	0.556×10^{-4}	0.1965	1.148	1.25	2.29	$4.2 \leqslant T \leqslant 120$ K
0.20	-0.105×10^{-4}	0.3817	5.607	1.75	2.76	$4.2 \leqslant T \leqslant 150$ K

Curie - Weiss law ($T>T^*$)						
x	χ_0 (emu mol^{-1})	C (emu K/mol-f.u.)	θ (K)	$\mu_{\rm eff}=g\sqrt{J(J+1)}\cong 2\sqrt{S(S+1)}$		Temperature
				(μ_B / mol-f.u.)	(μ_B / Cr-ion)	
0.00						
0.03	0.912×10^{-4}	0.07111	1.74	0.754	3.08	$205 \leqslant T \leqslant 460$ K
0.05	-0.144×10^{-3}	0.2781	-141	1.49	4.72	$200 \leqslant T \leqslant 300$ K
0.08	-0.129×10^{-3}	0.3457	-116	1.66	4.16	$210 \leqslant T \leqslant 340$ K
0.10	-0.127×10^{-4}	0.3280	-52.9	1.62	3.62	$250 \leqslant T \leqslant 650$ K
0.15	-0.251×10^{-3}	0.5856	-51.3	2.16	3.95	$350 \leqslant T \leqslant 650$ K
0.20	-0.505×10^{-4}	0.5864	-0.384	2.17	3.42	$260 \leqslant T \leqslant 650$ K

position region $0.08 \leqslant x \leqslant 0.20$ exhibits these broad humps in χ at the almost constant temperature 180 K, which corresponds to the change from the metallic to semiconductive behavior, as shown in Fig. 8. As can be seen in Table I, there is a significant difference in the magnitude of μ_{eff} between above and below $T^\star$. The ionic state of the Cr^{3+} ion undergoes the spin crossover phenomenon around $T^\star$, which comes from a change in the quantum state of the electron spin for Cr^{3+}. Below $T^\star$, the local crystal distortion at the B site may split the t_{2g} level into lower symmetry and then the low-spin state (not in 10 Dq but only in the t_{2g} subspace) is realized within the t_{2g} subspace for the Cr^{3+} ion with $s=1/2$, where the e_g state is neglected because of the much higher energy level.

As can be seen in Table I, a crude evaluation can lead to a conclusion that the spin values of the Cr^{3+} ion are $s=3/2$ and 1/2 above and below $T^\star$, respectively, in the intermediate composition region $0.08 \leqslant x \leqslant 0.20$. The Weiss temperature θ is very low for the region $T \leqslant T^\star$. It is interesting, however, that the magnitude of θ, with an antiferromagnetic coupling for $T \geqslant T^\star$, indicates a systematic decrease with increasing x. The metallic state is essentially attained for $T \geqslant T^\star$ in $0.08 \leqslant x \leqslant 0.20$. When the value of x approaches the ferromagnetic state of $x \geqslant 0.25$, θ drops abruptly to zero.

The specimens with $x \geqslant 0.25$ exhibit ferromagnetism. The magnetic properties of the ferromagnetic composition region are summarized in Tables II and III. Here the value of the magnetic moment n_B is defined to be $n_B \cong gs$ in units of μ_B, which is obtained from the value of magnetization at 4.2 K

TABLE II. Summary of the magnetic properties of $Cu(Ir_{1-x}Cr_x)_2S_4$ for $0.25 \leqslant x \leqslant 1.00$. The value n_B/Cr-ion, in the Bohr magneton number, indicates that only Cr ions possess a localized magnetic moment.

Magnetization ($T=4.2$ K, $H=10$ kOe)			
x	$\sigma_{\rm m}$ (emu / mol)	$n_{\rm B}$ / mol-f.u.	$n_{\rm B}$ / Cr-ion
0.25	2045.8	0.366	0.733
0.30	2652.1	0.475	0.791
0.40	6310.0	1.13	1.41
0.50	9172.4	1.64	1.64
0.60	13062	2.34	1.95
0.70	15352	2.75	1.96
0.80	18073	3.24	2.02
1.00	22543	4.04 [a]	2.02

[a]In other results, 4.58 in Ref. 56, 3.9 in Ref. 64, 4.79 in Ref. 65, and 4.85 in Ref. 67.

TABLE III. Summary of the magnetic properties of $Cu(Ir_{1-x}Cr_x)_2S_4$ for $0.25 \leqslant x \leqslant 1.00$. The notations are the same as given in Table I.

Curie - Weiss law					
x	C (emu K/mol-f.u.)	θ_p (K)	$\mu_{\rm eff} = g\sqrt{J(J+1)} \cong 2\sqrt{S(S+1)}$		Temperature
			(μ_B / mol-f.u.)	(μ_B / Cr-ion)	
0.25	0.7247	39	2.41	3.41	$185 \leqslant T \leqslant 350$ K
0.30	0.7153	42	2.39	3.09	$90 \leqslant T \leqslant 300$ K
0.40	1.014	106	2.85	3.18	$140 \leqslant T \leqslant 340$ K
0.50	1.299	138	3.22	3.22	$155 \leqslant T \leqslant 340$ K
0.60	1.658	189	3.64	3.32	$245 \leqslant T \leqslant 340$ K
0.70	1.814	222	3.81	3.22	$260 \leqslant T \leqslant 340$ K
0.80	3.421	253	5.23	4.14	$280 \leqslant T \leqslant 340$ K

in 10 kOe. The magnitude of the n_B/Cr ion is only half the value of $s=3/2$ expected from the Curie-Weiss law $T \geqslant T_c$. The magnetization is not saturated at 10 kOe. A possible mechanism such as weak ferromagnetism originating from a noncollinear spin alignment may be considered. The degree of the noncolinear spin alignment increases with decreasing x from $x=1.0$, which is seen in Tables II and III. The magnetic moment n_B/Cr-ion is found to be 2.02 for the single crystal of $CuCr_2S_4$ in our measurement. Therefore, the formula unit of $CuCr_2S_4$ has a net magnetic moment of $4.04\mu_B$, which is less than $5.0\mu_B$.

E. Phase diagram of $Cu(Ir_{1-x}Cr_x)_2S_4$

Figure 16 provides a phase diagram between temperature versus Cr composition x. For $0.03<x<0.08$, the coexistence of cubic and tetragonal phases has been observed below $T_{M\text{-}I}$. The sharp M-I transition is seen only for $x \leqslant 0.05$. The resistive jump smears out, then the critical value of the M-I transition becomes ill defined around $x=0.08$. For $0.10<x<0.80$, the resistivity indicates a semiconductive behavior without any anomaly. The resistivity recovers the metallic temperature dependence for the specimens with $x \geqslant 0.80$.

Solid circles for $x \geqslant 0.20$ show the asymptotic ferromagnetic Curie temperature θ_p. The value of θ_p increases almost linearly with increasing x. The ferromagnetic state disappears at the critical composition $x_c=0.20$. The statistical theory on the basis of cluster variation method by Sato *et al.*[78] predicts $x_c=0.25$; here a dilute ferromagnet of an Ising spin system is assumed with the number of nearest neighbor $z=6$. The composition dependence of θ_p and the value of x_c are fairly close to the result of this theory.

The intermediate composition region is found between $0.08<x<0.20$, where neither a M-I nor ferromagnetic transition takes place. The crystal symmetry remains cubic; nev-

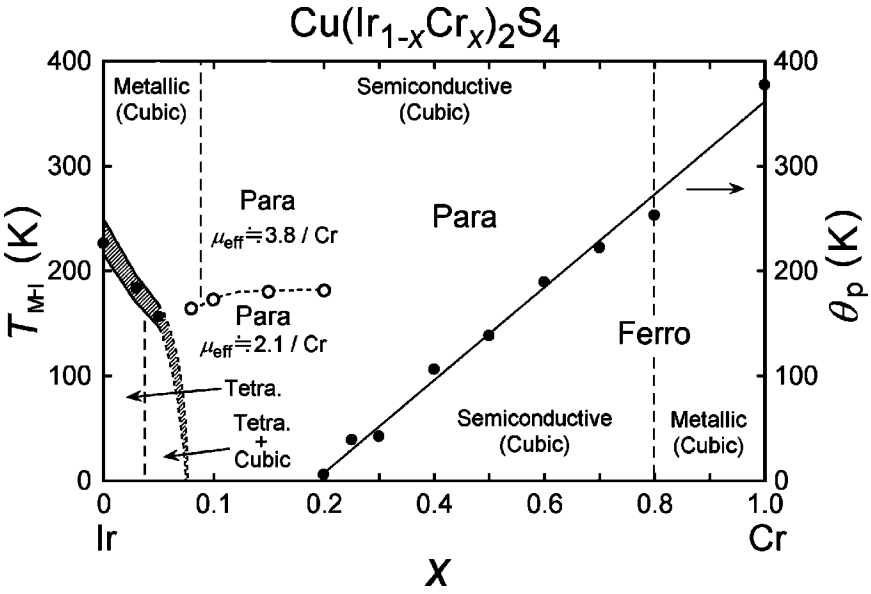

FIG. 16. A phase diagram of $Cu(Ir_{1-x}Cr_x)_2S_4$ for temperature versus composition x. The solid circles indicate the M-I transition temperature $T_{M\text{-}I}$ for $x<0.08$, which corresponds fairly well to the step-like anomaly in the susceptibility and the structural transformation. The asymptotic ferromagnetic Curie temperature θ_p decreases linearly with decreasing x.

ertheless, the *B*-site local distortion may occur around $T^{\star} \cong 180$ K, which is less sensitive to the composition. The hump shaped anomaly is observed in the magnetic susceptibility around $T^{\star}$. Above and below $T^{\star}$, the values of the effective magnetic moment are largely different from each other. The values are μ_{eff}/Cr atom$\cong 3.8$ and 2.1, respectively. The spin state may be changed from $s=3/2$ at higher temperature to $s=1/2$ at lower temperature. The energy level t_{2g} at the *B* site splits into lower symmetry. Then the low-spin state within the t_{2g} subspace (not in 10 Dq) is realized for a Cr^{3+} ion with $s=1/2$. The magnetic state of the Cr^{3+} ion indicates a crossover from a high temperature $s=3/2$ state to low temperature $s=1/2$ state around $T^{\star}$.

Finally, we should like to point out that the magnetic moments of Cu and Ir ions have been neglected in our analysis. Nevertheless, it is natural to extract the conclusion that Cu ions at tetrahedral sites are occupied by not divalent but monovalent states. Otherwise, the value of effective magnetic moment per Cr ion, which is extracted from the Curie-Weiss law, should be extremely large because our analysis attributes the source of all the magnetic moments to Cr ions, which has not been found in our measurements in Tables (I–III). Furthermore, any sign of a ferrimagnetic behavior with a characteristic curvature in $1/\chi$ for a temperature not much above T_C is also not found. Our results for $1/\chi$ show-completely straight lines presented in Fig. 15, which are characteristic of a ferromagnet. The curvature of the plot of $1/\chi$ versus T in the ferrimagnet should exhibit a characteristic asymptotic behavior if the Cu ion is in a divalent state, having $s=1/2$ antiparallel to the Cr spins. Consequently, the global magnetic aspects of our experimental results strongly support Lotgering's picture of the spin configuration as $Cu^{+}Cr^{3+}Cr^{4+}S_4^{2-}$,[56,57,64,72,76] which is completely different from Goodenough's model of $Cu^{2+}Cr_2^{3+}S_4^{2-}$.[61,63] It is our hope that fruitful discussion will be given on the basis of the present study.

ACKNOWLEDGMENTS

The present research was supported financially by a Grant-in Aid for Scientific Research (No.12046204)) from the Ministry of Education, Science, Sports, and Culture of Japan. Financial support by the CASIO Science Promotion Foundation's Research Grant (Tokyo, No. H14-Ac-2)) is also gratefully acknowledged.

*Author to whom correspondence should be addressed. Electronic address: naga-sho@mmm.muroran-it.ac.jp

[1] S. Nagata, T. Hagino, Y. Seki, and T. Bitoh, Physica B **194-196**, 1077 (1994).
[2] T. Furubayashi, T. Matsumoto, T. Hagino, and S. Nagata, J. Phys. Soc. Jpn. **63**, 3333 (1994).
[3] T. Hagino, Y. Seki, and S. Nagata, Physica C **235-240**, 1303 (1994).
[4] T. Hagino, T. Tojo, T. Atake, and S. Nagata, Philos. Mag. B **71**, 881 (1995).
[5] G. Oomi, T. Kagayama, I. Yoshida, T. Hagino, and S. Nagata, J. Magn. Magn. Mater. **140-144**, 157 (1995).
[6] T. Oda, M. Shirai, N. Suzuki, and K. Motizuki, J. Phys.: Condens. Matter **7**, 4433 (1995).
[7] K. Kumagai, S. Tsuji, T. Hagino, and S. Nagata, in *Spectroscopy of Mott Insulators and Correlated Metals*, edited by A. Fujimori and Y. Tokura, Springer Series in Solid-State Sciences, Vol. 119 (Springer-Verlag, Berlin, 1995), p. 255.
[8] S. Nagata, S. Yasuzuka, Y. Kato, T. Hagino, M. Matsumoto, N. Kijima, and S. Ebisu, Czech. J. Phys. **46**, Suppl. S5, 2425 (1996).
[9] P. Somasundaram, J. M. Honig, T. M. Pekarek, and B. C. Crooker, J. Appl. Phys. **79**, 5401 (1996).
[10] T. Furubayashi, T. Kosaka, J. Tang, T. Matsumoto, Y. Kato, and S. Nagata, J. Phys. Soc. Jpn. **66**, 1563 (1997).
[11] J. Matsuno, T. Mizokawa, A. Fujimori, D. A. Zatsepin, V. R. Galakhov, E. Z. Kurmaev, Y. Kato, and S. Nagata, Phys. Rev. B **55**, R15979 (1997).
[12] S. Tsuji, K. Kumagai, N. Matsumoto, Y. Kato, and S. Nagata, Physica B **237-238**, 156 (1997).
[13] S. Tsuji, K. Kumagai, N. Matsumoto, and S. Nagata, Physica C **282-287**, 1107 (1997).
[14] F. A. Chudnovskii, A. L. Pergament, G. B. Stefanovich, P. Somasundaram, and J. M. Honig, Phys. Status Solidi A **162**, 601 (1997).
[15] P. Somasundaram, D. Kim, J. M. Honig, and T. M. Pekarek, J. Appl. Phys. **81**, 4618 (1997).
[16] H. Kang, P. Mandal, I. V. Medvedeva, K. Bärner, A. Poddar, and E. Gmelin, Phys. Status Solidi A **163**, 465 (1997).
[17] E. Z. Kurmaev *et al.*, Solid State Commun. **108**, 235 (1998).
[18] S. Nagata, N. Matsumoto, Y. Kato, T. Furubayashi, T. Matsumoto, J. P. Sanchez, and P. Vulliet, Phys. Rev. B **58**, 6844 (1998).
[19] J. Tang, T. Matsumoto, T. Furubayashi, T. Kosaka, S. Nagata, and Y. Kato, J. Magn. Magn. Mater. **177-181**, 1363 (1998).
[20] J. Tang, T. Furubayashi, T. Kosaka, S. Nagata, Y. Kato, H. Asano, and T. Matsumoto, Rev. High Pressure Sci. Technol. **7**, 496 (1998).
[21] H. Kang, K. Bärner, I. V. Medvedeva, P. Mandal, A. Poddar, and E. Gmelin, J. Alloys Compd. **267**, 1 (1998).
[22] P. Somasundaram, D. Kim, J. M. Honig, T. M. Pekarek, T. Gu, and A. I. Goldman, J. Appl. Phys. **83**, 7243 (1998).
[23] H. Kang, P. Mandal, I. V. Medvedeva, J. Liebe, G. H. Rao, K. Bärner, A. Poddar, and E. Gmelin, J. Appl. Phys. **83**, 6977 (1998).
[24] K. Balcerek, Cz. Marucha, R. Wawryk, T. Tyc, N. Matsumoto, and S. Nagata, Philos. Mag. B **79**, 1021 (1999).
[25] N. Matsumoto, R. Endoh, S. Nagata, T. Furubayashi, and T. Matsumoto, Phys. Rev. B **60**, 5258 (1999).
[26] J. Tang, T. Matsumoto, T. Naka, T. Furubayashi, S. Nagata, and N. Matsumoto, Physica B **259-261**, 857 (1999).
[27] R. Oshima, H. Ishibashi, K. Tanioka, and K. Nakahigashi, in *Proc. the Int. Conf. on Solid-Solid Phase Transformations '99 (JIMIC-3)*, edited by M. Koiwa, K. Otsuka, T. Miyazaki (The Japan Institute of Metals, Sendai, 1999), p. 895.
[28] H. Suzuki, T. Furubayashi, G. Cao, H. Kitazawa, A. Kamimura, K. Hirata, and T. Matsumoto, J. Phys. Soc. Jpn. **68**, 2495 (1999).
[29] A. T. Burkov, T. Nakama, K. Shintani, K. Yagasaki, N. Matsumoto, and S. Nagata, Phys. Rev. B **61**, 10049 (2000).
[30] A. T. Burkov, T. Nakama, K. Shintani, K. Yagasaki, N. Matsu-

moto, and S. Nagata, Physica B **281-282**, 629 (2000).
[31] N. Matsumoto and S. Nagata, J. Cryst. Growth **210**, 772 (2000).
[32] M. Hayashi, M. Nakayama, T. Nanba, T. Matsumoto, J. Tang, and S. Nagata, Physica B **281-282**, 631 (2000).
[33] K. Kumagai, K. Kakuyanagi, R. Endoh, and S. Nagata, Physica C **341-348**, 741 (2000).
[34] Y. Kishimoto, T. Ohno, S. Nagata, N. Matsumoto, T. Kanashiro, Y. Michihiro, and K. Nakamura, Physica C **281-282**, 634 (2000).
[35] A. Goto, T. Shimizu, G. Cao, H. Suzuki, H. Kitazawa, and T. Matsumoto, Physica C **341-348**, 737 (2000).
[36] G. Cao, H. Suzuki, T. Furubayashi, H. Kitazawa, and T. Matsumoto, Physica B **281-282**, 636 (2000).
[37] G. L. W. Hart, W. E. Pickett, E. Z. Kurmaev, D. Hartmann, M. Neumann, A. Moewes, D. L. Ederer, R. Endoh, K. Taniguchi, and S. Nagata, Phys. Rev. B **61**, 4230 (2000).
[38] H. Kang, K. Bärner, H. Rager, U. Sondermann, P. Mandal, I. V. Medvedeva, and E. Gmelin, J. Alloys Compd. **306**, 6 (2000).
[39] J. Tang, T. Kikekawa, J. Z. Hu, J. F. Shu, H. K. Mao, T. Furubayashi, A. Matsushita, T. Matsumoto, S. Nagata, and N. Matsumoto, in *Proc. the Int. Conf. on Science and Technology of High Pressure, (AIRAPT-17)*, edited by M. H. Manghnani, W. J. Nellis, and M. F. Nicol (University Press, Hyderabad, 2000), p. 506.
[40] H. Ishibashi, T. Sakai, and K. Nakahigashi, J. Magn. Magn. Mater. **226-230**, 233 (2001).
[41] N. Matsumoto, Y. Yamauchi, J. Awaka, Y. Kamei, H. Takano, and S. Nagata, Int. J. Inorg. Mater. **3**, 791 (2001).
[42] W. Sun, T. Kimoto, T. Furubayashi, T. Matsumoto, S. Ikeda, and S. Nagata, J. Phys. Soc. Jpn. **70**, 2817 (2001).
[43] K. Oikawa, T. Matsumoto, T. Furubayashi, N. Matsumoto, and S. Nagata, J. Phys. Soc. Jpn. **70**, Suppl. A106 (2001).
[44] A. Goto, T. Shimizu, G. Cao, H. Suzuki, H. Kitazawa, and T. Matsumoto, J. Phys. Soc. Jpn. **70**, 9 (2001).
[45] R. Endoh, N. Matsumoto, S. Chikazawa, S. Nagata, T. Furubayashi, and T. Matsumoto, Phys. Rev. B **64**, 075106 (2001).
[46] G. Cao, T. Furubayashi, H. Suzuki, H. Kitazawa, T. Matsumoto, and Y. Uwatoko, Phys. Rev. B **64**, 214514 (2001).
[47] K. Yagasaki, T. Nakama, M. Hedo, A. T. Burkov, N. Matsumoto, and S. Nagata, J. Magn. Magn. Mater. **226-230**, 244 (2001).
[48] P. G. Radaelli, Y. Horibe, M. J. Gutmann, H. Ishibashi, C. H. Chen, R. M. Ibberson, Y. Koyama, Y-S. Hor, V. Kiryukhin, and S-W. Cheong, Nature (London) **416**, 155 (2002).
[49] R. Endoh, N. Matsumoto, J. Awaka, S. Ebisu, and S. Nagata, J. Phys. Chem. Solids **63**, 669 (2002).
[50] K. Yagasaki, T. Nakama, M. Hedo, K. Uchima, Y. Shimoji, N. Matsumoto, S. Nagata, H. Okada, H. Fujii, and A. T. Burkov, J. Phys. Chem. Solids **63**, 1051 (2002).
[51] S. Nagata, S. Ito, R. Endoh, and J. Awaka, Philos. Mag. B **82**, 1679 (2002).
[52] H. Ishibashi, T. Y. Koo, Y. S. Hor, A. Borissov, P. G. Radaelli, Y. Horibe, S. W. Cheong, and V. Kiryukhin, Phys. Rev. B **66**, 144424 (2002).
[53] S. Nagata, N. Matsumoto, R. Endoh, and N. Wada, Physica B **329–333**, 944 (2003).
[54] T. Furubayashi, H. Suzuki, T. Matsumoto, and S. Nagata, Solid State Commun. **126**, 617 (2003).
[55] H. Hahn, C. de Lorent, and B. Harder, Z. Anorg. Allg. Chem. **283**, 138 (1956).
[56] F. K. Lotgering, in *Proc. the Int. Conf. on Magnetism, Nottingham* (Institute of Physics and Physical Society, London, 1964), p. 533.
[57] F. K. Lotgering, Solid State Commun. **2**, 55 (1964).
[58] R. J. Bouchard, P. A. Russo, and A. Wold, Inorg. Chem. **4**, 685 (1965).
[59] P. M. Raccah, R. J. Bouchard, and A. Wold, J. Appl. Phys. **37**, 1436 (1966).
[60] M. Robbins, H. W. Lehmann, and J. G. White, J. Phys. Chem. Solids **28**, 897 (1967).
[61] J. B. Goodenough, Solid State Commun. **5**, 577 (1967).
[62] K. Ohbayashi, Y. Tominaga, and S. Iida, J. Phys. Soc. Jpn. **24**, 1173 (1968).
[63] J. B. Goodenough, J. Phys. Chem. Solids **30**, 261 (1969).
[64] R. P. van Stapele and F. K. Lotgering, J. Phys. Chem. Solids **31**, 1547 (1970).
[65] T. Kanomata, H. Ido, and T. Kaneko, J. Phys. Soc. Jpn. **29**, 332 (1970).
[66] M. Robbins, A. Menth, M. A. Miksovsky, and R. C. Sherwood, J. Phys. Chem. Solids **31**, 423 (1970).
[67] E. Riedel and E. Horváth, Z. Anorg. Allg. Chem. **399**, 219 (1973).
[68] K. P. Belov, Yu. D. Tret'yakov, I. V. Gordeev, L. I. Koroleva, A. V. Ped'ko, E. I. Smirnovskaya, V. A. Alferov, and Yu. G. Saksonov, Fiz. Tverd. Tela (Leningrad) **14**, 2155 (1972) [Sov. Phys. Solid State **14**, 1862 (1973)].
[69] E. Riedel and E. Horvath, Mater. Res. Bull. **8**, 973 (1973).
[70] H. Itoh, J. Phys. Soc. Jpn. **48**, 1130 (1980).
[71] J. Padiou, D. Bideau, and J. P. Troadec, J. Solid State Chem. **31**, 401 (1980).
[72] *Ferro-Magnetic Materials*, edited by E. P. Wohlfarth, A handbook on the properties of magnetically ordered substances Vol. 3 (North-Holland, Amsterdam, 1982), p 603.
[73] H. D. Lutz, U. Koch, and I. Okonska-kozlowska, J. Solid State Chem. **51**, 69 (1984).
[74] A. Kimura, J. Matsuno, J. Okabayashi, A. Fujimori, T. Shishidou, E. Kulatov, and T. Kanomata, Phys. Rev. B **63**, 224420 (2001).
[75] K. Oda, S. Yoshii, Y. Yasui, M. Ito, T. Ido, Y. Ohno, Y. Kobayashi, and M. Sato, J. Phys. Soc. Jpn. **70**, 2999 (2001).
[76] J. Krok-Kowalski, J. Warczewski, and K. Nikiforov, J. Alloys Compd. **315**, 62 (2001).
[77] S. Nagata (private communication).
[78] H. Sato, A. Arrott, and R. Kikuchi, J. Phys. Chem. Solids **10**, 19 (1959).